ELSEVIER

Contents lists available at ScienceDirect

Bioresource Technology

journal homepage: www.elsevier.com/locate/biortech





The effect of additional salinity on performance of a phosphate buffer saline buffered three-electrode bioelectrochemical system inoculated with wastewater

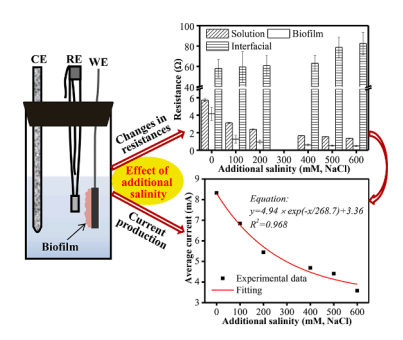
Fei Guo^{a,b,*}, Jerome T. Babauta^b, Haluk Beyenal^b

- ^a School of Civil Engineering, Architecture and Environment, Xihua University, Chengdu 610039, China
- ^b The Gene and Linda Voiland School of Chemical Engineering and Bioengineering, Washington State University, Pullman, WA, USA

HIGHLIGHTS

- Increased additional salinity decreased current generation in a PBS-buffered RES
- Additional salt addition changed the composition distribution of total resistance.
- Interfacial resistance accounted for 85%–97.8% of the total resistance.
- Decreased current was mainly resulted from the increased interfacial resistance.
- The optimal additional salinity for acetate degradation was 200 mM NaCl.

G R A P H I C A L A B S T R A C T



ARTICLE INFO

Keywords:
Bioelectrochemical system
PBS-buffered substrate
Additional salinity
Current production
Electrochemical impedance spectroscopy
Interfacial resistance

ABSTRACT

In bioelectrochemical system (BES), phosphate buffer saline (PBS) is usually used to achieve a suitable pH condition, which also increases electrolyte salinity. A series of factors that change with salinity will affect BES performance. To simplify the scenario, a three-electrode BES is used to investigate how additional salinity affects the performance of a 50 mM PBS-buffered BES. Results demonstrated that current production decreased with increasing salinity and the dominant exoelectrogens were not inhibited with the addition of 200 mM NaCl. The distribution of system resistance was analyzed by electrochemical impedance spectroscopy. Compared to the decreased solution and biofilm resistance, the increased interfacial resistance that accounted for up to 97.8% of total resistance was the dominant reason for the decreased current production with the increasing additional salinity. The effects of additional salinity on acetate degradation and columbic efficiency were also analyzed.

1. Introduction

The bioelectrochemical system (BES) is a biologically catalyzed electrochemical technology for bioenergy recovery and wastewater

treatment, which mainly includes microbial fuel cells (MFCs), microbial desalination cells (MDCs), microbial electrolysis cells (MECs), and three-electrode bioelectrochemical reactors. Substrate salinity or conductivity is a critical factor that regulates the performance of BES (Guo et al.,

^{*} Corresponding author at: School of Civil Engineering, Architecture and Environment, Xihua University, Chengdu 610039, China. *E-mail address*: fei.guo@mail.xhu.edu.cn (F. Guo).

2020). A solution conductivity of \sim 20 mS/cm was suggested for a typical maximum power density in MFCs (Logan and Rabaey, 2012). However, the conductivity of the raw domestic wastewater is around 1.8 mS/cm, which can be increased to 8.1 \pm 0.3 mS/cm after an adjusted with 50 mM PBS (Liu et al., 2011). There is a wide gap in substrate conductivity between the suggested optimal and real conditions.

To narrow the conductivity gap, salt (e.g., NaCl or KCl) or phosphate buffer saline (PBS) is usually added to the electrolyte in MFCs, which can decrease electrolyte resistance and improve power performance of MFCs (Adelaja et al., 2015; Lefebvre et al., 2012; Liu et al., 2005; Miyahara et al., 2016). Increasing substrate salinity also decreases membrane resistance and improves catalyst performance at the cathode in MFCs. For example, an increased NaCl concentration dramatically decreased the resistance of anion and cation exchange membranes, especially when NaCl concentration was lower than 0.1 M (Dlugolecki et al., 2010a, 2010b). It was reported that higher salt concentration reduced platinum activity in the oxygen reduction reaction, while improved cobalt tetramethoxyphenyl porphyrin (CoTMPP) catalyst performance (Wang et al., 2011).

Compared to MFCs, the simple configuration of a three-electrode BES, with no membrane or cathodic catalyst, makes it much easier to analyze how additional salt influences the current production. For example, researchers added 517 mM, 776 mM, and 1034 mM NaCl (30 g/L, 45 g/L, and 60 g/L) into the BES electrolyte, and analyzed the current production and bacterial community structure (Rousseau et al., 2013, 2014). In another BES enriched with Geobacter sulfurreducens, current generation was improved with NaCl concentrations increased from 0 mM to 200 mM (Harrington et al., 2015). However, increasing the electrolyte salinity does not necessarily lead to an improved BES performance. In a single-chamber microbial electrolytic cell (threeelectrode BES), adding 100 mM NaCl into a 50 mM PBS-buffered electrolyte did not increase current density, since there was a decreased buffer migration resulting from NaCl addition (Torres et al., 2008). A decreased buffer capacity was also suggested when 100 mM KCl was added to a PBS-buffered electrolyte, although it decreased ohmic drop (Oliot et al., 2016).

It was reported that the maximum performance of MFCs was obtained at a relatively low NaCl concentration of 1% (w/v) or 0.1 M, and further salt addition would increase internal resistance and decrease power density (Adelaja et al., 2015; Miyahara et al., 2015). More recently, 10 mM NaCl addition was demonstrated as the optimal dosage for current production in H-type microbial electrolysis cells (Lusk et al., 2016). The minimally increased power output could be due to the deteriorated buffer migration, and inhibited bacterial activity when the salt is added to the medium. It should be noted that PBS and bicarbonate not only buffer pH condition, but improve electrolyte ionic conductivity. The salt addition does not lead to a better power performance, probably because neither ionic strength nor electrolyte conductivity are controlling factors in MFCs with 50 mM PBS (Feng et al., 2008; Nam et al., 2010). In addition, it was suggested that the solution conductivity originated from buffer were more important than the buffer itself given relatively stable pH condition (Nam et al., 2010).

While there are reports on power performance improvement by the addition of salts, researchers failed to investigate the changes in resistance of each individual component of MFCs or three-electrode BES using electrochemical techniques such as electrochemical impedance spectroscopy (EIS) (Harrington et al., 2015; Lefebvre et al., 2012; Liu et al., 2005; Miyahara et al., 2015, 2016; Rousseau et al., 2013, 2014; Vijay et al., 2018). It is important to understand the distribution of the total resistance and how it changes as the electrolyte salinity increases, which enables us to obtain optimal performance with the lowest salt addition. It is also important to investigate how current is changing as the additional salinity is supplemented in a PBS-buffered BES, which should be better evaluated in multiple aspects.

In the present work, the effect of additional salinity on performance of a 50 mM PBS-buffered three-electrode BES was investigated. Salt was

supplemented to achieve concentrations from 0 to 600 mM NaCl in a PBS-buffered medium. Current production at each NaCl concentration was collected. Cyclic voltammetry (CV) and its first derivative were used to analyze the metabolic activity and electron transfer rate of electrochemically active bacteria (EAB). EIS was used to determine the resistance of each individual component, including the solution resistance, biofilm resistance, and interfacial resistance, which helped for explaining the changes in current generation with additional salinity. Finally, the acetate removal rates and columbic efficiencies at different salinities were also analyzed. The findings in this work will provide suggestions on power performance improvement in BES.

2. Materials and methods

2.1. Three-electrode bioelectrochemical reactor

A cylindrical three-electrode BES reactor with a working volume of 185 mL was constructed as previously described (Guo et al., 2018). The working electrode was a piece of graphite felt with dimensions of 3.5 cm \times 3.0 cm \times 0.5 cm. The counter electrode was a graphite rod (Sigma-Aldrich, catalog#: 496545) with diameter of 6 mm. An Ag/AgCl reference (+197 mV, νs Standard hydrogen electrode, SHE) was used as reference electrode that was placed next to the working electrode. Norprene tubing (Cole-Parmer, catalog #: EW-06404-14 and EW-06404-16) was used to feed medium and to discharge waste medium.

2.2. Inoculum and reactor medium

Anaerobic activated sludge (25 mL) was used as inoculum for enriching working electrode. Reactor medium contains: sodium acetate, 1.64 g/L (20 mM); PBS, 50 mM (containing NaH₂PO₄·H₂O, 2.45 g/L; Na₂HPO₄, 4.58 g/L; NH₄Cl, 0.31 g/L; KCl, 0.13 g/L); salts solution (100×), 10 mL/L; Wolfe's vitamin solution (100×), 10 mL/L; and modified Wolfe's mineral solution (100×), 10 mL/L. Addition salinity of 0 mM, 100 mM, 200 mM, 400 mM, 500 mM, and 600 mM NaCl was added into medium in proper order, leading to solution conductivity of 8.3 mS/cm, 18.3 mS/cm, 29.2 mS/cm, 46.9 mS/cm, 55.4 mS/cm, and 6.31 mS/cm, respectively. The conductivity was determined by a multiparameter analyzer (DZS-708L, INESA, Shanghai). Medium pH was adjusted to 6.8–7.0. The medium was autoclaved at 121 °C for 20 min, and then sparged with a gas mixture of N₂ and CO₂ (80%/20%) until precipitated chemicals dissolved.

2.3. Start-up and operation

25~mL anaerobic active sludge and 160~mL defined medium were mixed well and used for start-up. The working electrode of the BES was polarized at 0.25~V vs Ag/AgCl using an Interface 1000~potentiostat (Gamry Instruments, Warminster, PA, USA). The BES was started up in batch mode and switched into continuous mode after reproducible current was observed. The substrate with different NaCl concentrations of 0 mM, 100~mM, 200~mM, 400~mM, 500~mM and 600~mM was continuously fed at a flow rate of 0.25~mL/min. Current was collected for 36~h at each NaCl concentration. At the end of each condition, CV, EIS and medium samples were collected. All experiments were conducted in an incubator at $30~^\circ\text{C}$. A magnetic stir was used to mix the medium in the BES throughout the experiment. The substrate in BES was continuously sparged with gas mixture of N_2 and CO_2 to maintain an anaerobic condition throughout the experiments.

2.4. Electrochemical analysis

Average current at different additional salinities was calculated using Eq. (1):

$$I_{ave} = \frac{\int_0^T idt}{T} \tag{1}$$

where i (mA) is the current, T (s) is the duration of current collected. At the end of experiment, CV was collected using a Gamry potentiostat (Interface1000, Gamry Instruments, Warminster, PA, USA), scanning from -0.7 V to 0.3 V vs Ag/AgCl at scanning rate of 10 mV per second. EIS experiments were conducted in duplicate using the same potentiostat with perturbation amplitude of 5 mV and the frequency varied from 1 MHz to 100 mHz. An equivalent electrical circuit (EEC) was used for EIS data fitting as previously described (Babauta and Beyenal, 2014). The EEC is composed of solution resistance (R1), biofilm resistance (R2), interfacial resistance (R3), and two constant phase elements (CPE) that model the total capacitive response of the biofilm at the different additional salinity. They are the biofilm CPE and the interfacial CPE with a corresponding CEP coefficient (Q) and exponential factor (α). The physical interpretation in detail has been described in the literature (Babauta and Beyenal, 2014). The Echem Analyst (Gamry Instruments, Warminster, PA) was used for fitting EIS data to the EEC and for obtaining Goodness of fit.

2.5. Acetate analysis and columbic efficiency

Inlet and outlet of BES reactor was collected for each NaCl concentration and acetate concentration was tested using HPLC (Agilent HPLC 1100 series, Agilent Technologies, CA, USA), following procedures described in the literature (Babauta et al., 2012). Acetate degradation rate was calculated using Eq. (2):

$$R = \Delta S^* Q / V \tag{2}$$

where ΔS is the difference in acetate concentration in inlet and outlet, Q is the flow rate (0.25 mL/min) as mentioned in Section 2.3, and V is the working volume of the reactor, 185 mL. Columbic efficiency (CE) was calculated using Eq. (3):

$$CE = \frac{\int_0^T i dt}{F^* b^* \Delta S^* Q^* T} \tag{3}$$

where F is Faraday's constant (96485 C/mol-e⁻); b=8, the number of moles of electrons generated per mole acetate; ΔS , Q, T has same meanings as described in Eqs. (1) and (2). Acetate degradation and CE was analyzed in duplicate for each salinity condition.

3. Results and discussion

3.1. Current production

After successful start-up, the concentration of additional salt in the medium gradually increased from 0 mM to 600 mM NaCl. As shown in Fig. 1, current decreased with the increase in NaCl concentrations, and a negative correlation was demonstrated (P < 0.005). After 36 h, the average current production was 8.32 mA (0 mM), 6.84 mA (100 mM), 5.44 mA (200 mM), 4.69 mA (400 mM), 4.41 mA (500 mM) and 3.58 mA (600 mM). In general, increased salinity decreased the current performance of the PBS-buffered three-electrode BES in this work.

Various findings were reported in BES operated under different salinities. In general, as NaCl concentrations increased, power output or current could be increased in PBS-buffered MFCs (Adelaja et al., 2015; Lefebvre et al., 2012; Liu et al., 2005), or in non-buffered MFCs (Miyahara et al., 2015). In buffered three-electrode BES reactors, current production was also increased with increases in salt concentration (Harrington et al., 2015). However, current density almost remained unchanged with increased salinity in buffered MECs (Lusk et al., 2016; Torres et al., 2008). Recently, it was also demonstrated that the background salinities, with no additional salt added, were the optimal conditions to obtain the highest voltage output in single-chamber MFCs

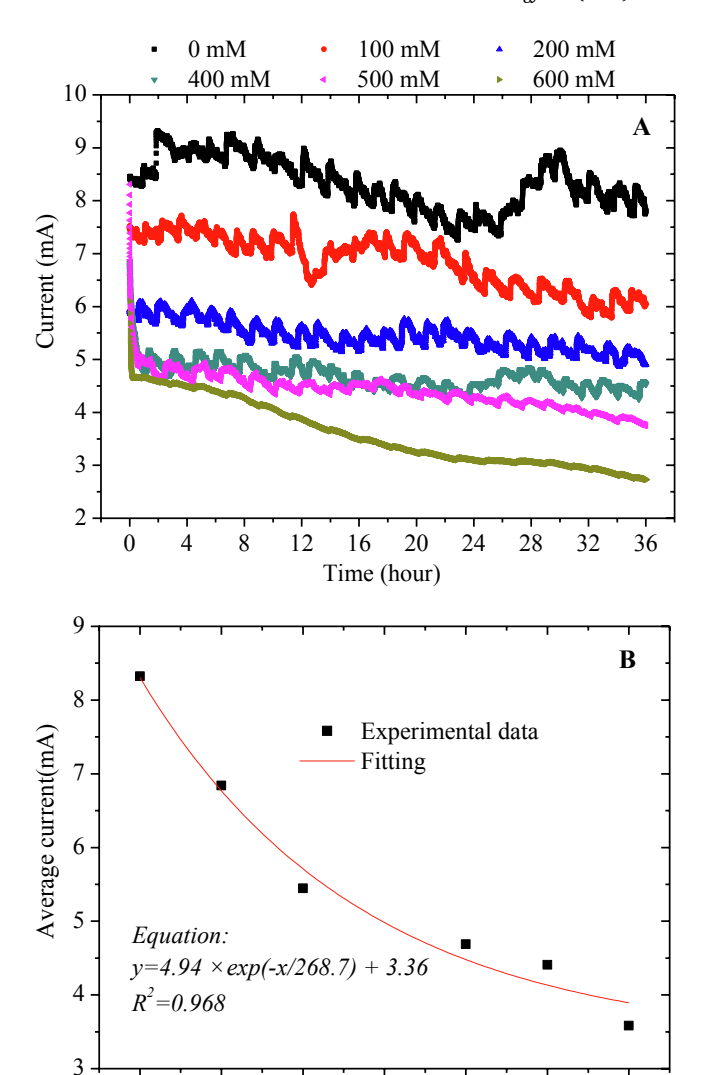


Fig. 1. Current production in PBS-buffered BES with working electrode polarized at 0.25 V *vs* Ag/AgCl (A), and average current over a 36-hour period at different additional salinity and its exponential fitting (B), *y*: current (mA), *x*: additional salinity (mM).

300

Additional salinity (mM, NaCl)

400

500

600

200

0

100

(Tan et al., 2019; Zeng et al., 2020). This study suggested that increasing electrolyte salinity does not necessarily lead to an increased power performance, especially in PBS-buffered BES.

Unlike the widely reported findings, increasing salinity decreased the current production in the present work. The opposite finding could be explained as follows. First, the improved performance in MFCs was attributed to the decreased internal resistance (Lefebvre et al., 2012; Liu et al., 2005). Internal resistance was composed of anodic resistance, cathodic resistance, membrane resistance, and electrolyte resistance (Fan et al., 2008). Specifically, it was the decreased membrane resistance and electrolyte resistance that finally improved power output (Lefebvre et al., 2012; Liu et al., 2005). But in a three-electrode BES with different configuration from MFCs, no membrane or separator was used, so the positive effect of the additional salinity on the membrane performance was not available in BES. Second, it has been demonstrated that a salinity increase from 0.6% to 1.2% could increase cathode potential, leading to a higher overall voltage and power density (Zuo et al., 2006). BES has no cathode compartment and current production could not be enhanced by an increased cathode performance at higher salinity. Generally, the increased power output with the increase in additional salinity in MFCs is mainly ascribed to the decreased membrane resistance and better cathode performance, and the lower electrolyte resistance.

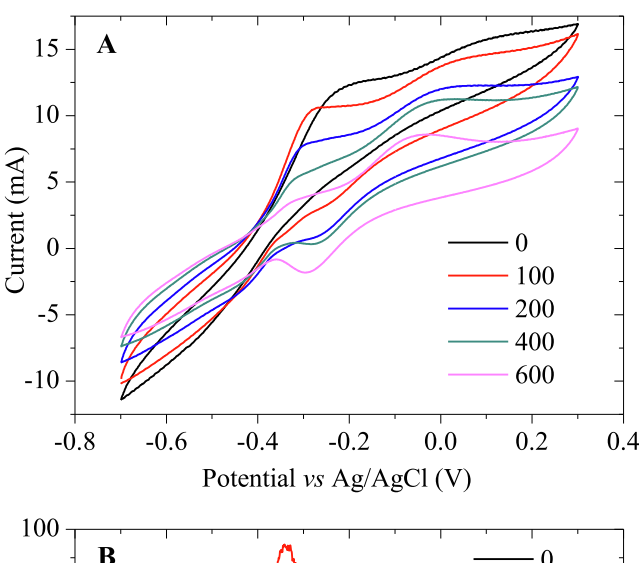
On the other hand, relatively low optimal salinity was also demonstrated in MFCs (Karthikeyan et al., 2016; Li et al., 2013; Miyahara et al., 2015). It could be due to the more positive anode potential resulting from the inhibition of bacterial activity by the relatively high additional salinity (Lefebvre et al., 2012; Zuo et al., 2006). It was suggested that increasing ionic conductivity does not necessarily lead to an increased MFC performance, as the background salinities were demonstrated to be the optimal conditions and the first dosage of additional salt decreased voltage output (Tan et al., 2019; Zeng et al., 2020). Furthermore, no buffer solution was used, nor was the total salinity accounted for in the literature (Karthikeyan et al., 2016; Li et al., 2013; Miyahara et al., 2015), indicating that the basic electrolyte without buffer solution was probably subjected to the insufficient ionic strength which could be improved by the additional salinity, and a better power performance was obtained. In the present work, the medium was buffered with 50 mM PBS, which enhanced ionic strength and decreased electrolyte resistance (Fan et al., 2008; Feng et al., 2008; Nam et al., 2010). Therefore, the electrolyte resistance was probably not a controlling factor and further additional salinity did not improve the current

In 50-mM PBS or bicarbonate-buffered MECs, the addition of NaCl did not significantly increase current production (Lusk et al., 2016; Torres et al., 2008). In the literature, a narrower salinity range from 0 mM to 50 mM or to 100 mM was observed. In the present work, the starting additional salinity was 100 mM NaCl, at which the current production was decreased compared to the 0 mM NaCl condition. It could be inferred that there was probably a missed turning point at the salinity between 0 mM and 100 mM. In the BES enriched with G. sulfurreducens, the increased current production with the increase in NaCl concentration was due to the decreased ion transport limitations (Harrington et al., 2015). The ion transport limitations could be resulted from the different buffer solution. For example, increasing bicarbonate concentration from 10 mM to 100 mM was helpful to obtaining a better current output (Lusk et al., 2016). The buffer in Harrington's work was 2 g/L sodium carbonate (~18.9 mM), suggesting the potential ion transport limitations resulted from the relatively low buffering capacity and ionic strength, which was improved by NaCl addition (Harrington et al., 2015). However, in a 50 mM PBS-buffered MEC, additional salinity failed to significantly increase current density, which suggested the different capacities of the buffer solution and various effects of additional salinity on BES performance (Harrington et al., 2015; Lusk et al., 2016; Torres et al., 2008). More importantly, the buffer performance may have been deteriorated with the additional salinity, leading to a decreased current production (Torres et al., 2008). Also, the decreased current could be due the shifted bacterial community at high additional salinity. It was demonstrated that salinity could change bacterial communities in non-buffered MFCs, and that G. sulfurreducens had the highest abundance ratio at salinity of 0.1 M NaCl (Miyahara et al., 2015, 2016). Recently, up to 1 M NaCl addition was suggested as the optimal salinity for power production in MFCs inoculated with bacterial consortium collected from the Sambhar Lake in India (Vijay et al., 2018). Therefore, the power performance and optimal salinity varies greatly with the BES reactor configuration, buffer solution, and inoculum sources.

3.2. Electrochemical analysis

3.2.1. Cyclic voltammetry analysis

For clarity, CV collected at 0 mM, 100 mM, 200 mM, 400 mM and 600 mM NaCl was plotted and analyzed (Fig. 2A). With the increase in additional salinity, peak current gradually decreased, suggesting the inhibition of salinity on EAB. The shape of CV was similar to that obtained in BES inoculated with domestic wastewater, and researchers



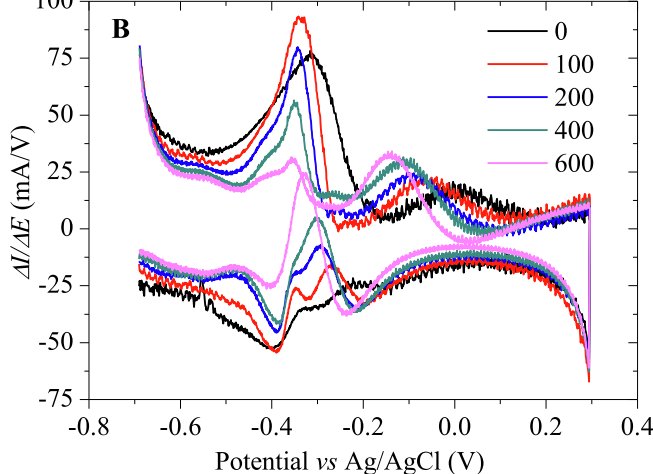


Fig. 2. Cyclic voltammetry (A), and the first derivative of cyclic voltammetry (B) in PBS-buffered BES at different additional salinity.

concluded the dominating role of *G. sulfurreducens* in power generation (Patil et al., 2010). There was also a similarity to CV of pure culture *G. sulfurreducens* (Srikanth et al., 2008).

The first derivatives of CV were calculated to analyze the redox systems, and the redox peaks represent the activity of EAB. As illustrated in Fig. 2B, there were two major redox systems, one centered at about -0.37 V vs Ag/AgCl (E_{f,1}), while for the other system, the midpoint potentials slightly shifted from -0.07 V at 0 mM NaCl to -0.19 V vs Ag/ AgCl at 600 mM NaCl (E_{f,2}). Especially, E_{f,1} was in good agreement with the redox couple observed in the wild type G. sulfurreducens biofilms with midpoint potentials centered at -0.15 V vs SHE (Marsili et al., 2008; Richter et al., 2009; Srikanth et al., 2008), and -0.376 V vs Ag/ AgCl (Fricke et al., 2008). The comparable peak heights of the redox couples centered at Ef.1 suggested that the bacterial activity of current production was not inhibited when additional salinity was increased from 0 mM to 200 mM NaCl (Fig. 2B). There should be other factors that decreased the current production in the BES. For example, electricityproducing bacteria other than the dominant EAB were inhibited by the NaCl addition, and the resistance distribution of the system probably changed with the NaCl addition, which will be discussed in Section 3.2.2

In the literature, it was demonstrated that the electron transfer from EAB to a solid electron acceptor was partially accomplished by cytochromes, such as periplasmic c-type cytochrome (PpcA), OmcB, OmcE, OmcS and OmcZ (Holmes et al., 2006; Nevin et al., 2009; Pessanha et al., 2006; Richter et al., 2009). The potential (Ef.1) was also comparable to

the midpoint potential of solubilized cytochromes involved in electron transfer in *G. sulfurreducens* biofilms: -0.1695 V or -0.167 V vs SHE for PpcA (Lloyd et al., 2003; Seeliger et al., 1998), -0.19 V vs SHE for OmcB purified from *G. sulfurreducens* (Magnuson et al., 2001). It was reported that OmcB was responsible for the electron transfer across the interface between electrode and *G. sulfurreducens* biofilms (Richter et al., 2009). One explanation for the decreased current production with the increase in salinity was that NaCl addition (higher than 200 mM) inhibited the activity of OmcB and thus resulted in an increase in electron transfer resistance at the biofilm/electrode interface (interfacial resistance, Section 3.2.2).

For the second redox system centered at $E_{\rm f,2}$, it could be concluded that EAB were not inhibited and even became more active with the increase in NaCl concentrations throughout the whole experiment. So, the species could adapt well to the high additional salinity, and some microorganisms had been demonstrated to be preferable to saline conditions (Pierra et al., 2015; Rousseau et al., 2014). So far, little work has been done reporting midpoint potentials ranging from $-0.07~\rm V$ to $-0.19~\rm V$ vs Ag/AgCl. The height of peaks of this redox system were much lower than that centered at $E_{\rm f,1}$. Moreover, redox systems centered at different potentials were suggested to play different roles in electron transfer (Fricke et al., 2008; Marsili et al., 2008).

3.2.2. Electrochemical impedance spectroscopy analysis

Representative impedance data was plotted (Fig. 3), and R1, R2, R3, Q1 and Q2 were calculated from EIS fittings. Goodness of fit for all parameters were 2.03×10^{-5} (0 mM), 6.28×10^{-5} (100 mM), 1.33×10^{-4} (200 mM), 1.67×10^{-4} (400 mM), 1.80×10^{-5} (500 mM), and 1.84×10^{-5} (600 mM), which were comparable to that reported in the literature (Babauta and Beyenal, 2014).

As shown in Fig. 4A, solution resistance (R1) dropped with the increase in salinity because of the enhanced ionic strength, a common approach used to improve power output in MFCs (Adelaja et al., 2015; Lefebvre et al., 2012; Liu et al., 2005; Miyahara et al., 2015). In the present work, solution resistance first experienced a fast decrease from $5.72 \pm 0.18~\Omega$ (0 mM) to $2.40 \pm 0.04~\Omega$ (200 mM), and then slowly decreased to $1.37 \pm 0.03~\Omega$ (600 mM). The results suggested that solution resistance would not keep decreasing with further addition of NaCl. So, it is impossible to obtain better performance by further adding NaCl after exceeding a threshold. On the contrary, power generation would deteriorate because of the inhibition to bacterial activity and plasmolysis (Rousseau et al., 2014). For example, Lefebvre et al. (2012) suggested that inhibition of electricity-producing bacteria began at 10 g/L

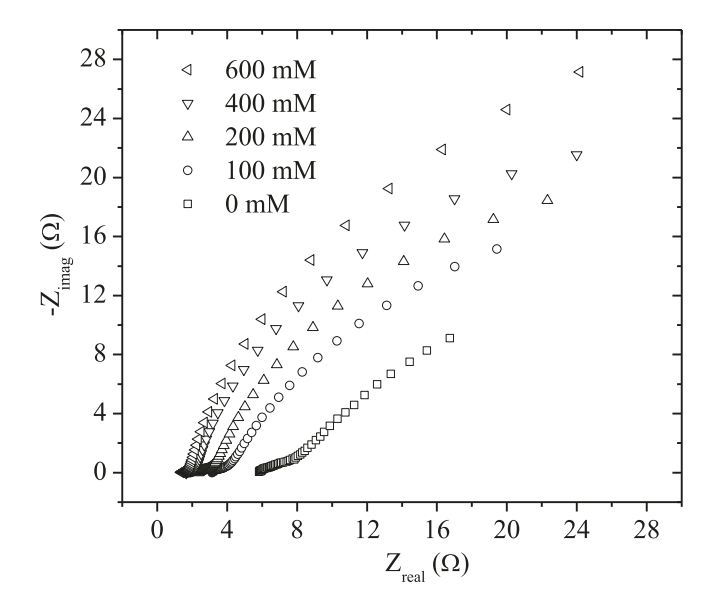
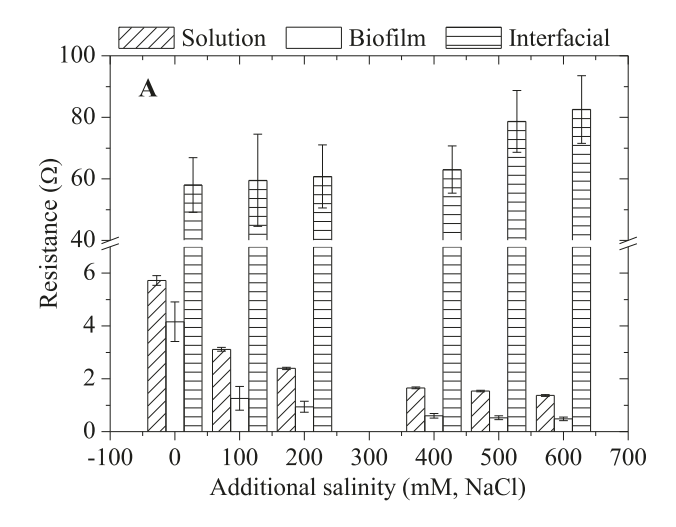


Fig. 3. Nyquist profiles in PBS-buffered BES at different additional salinity.



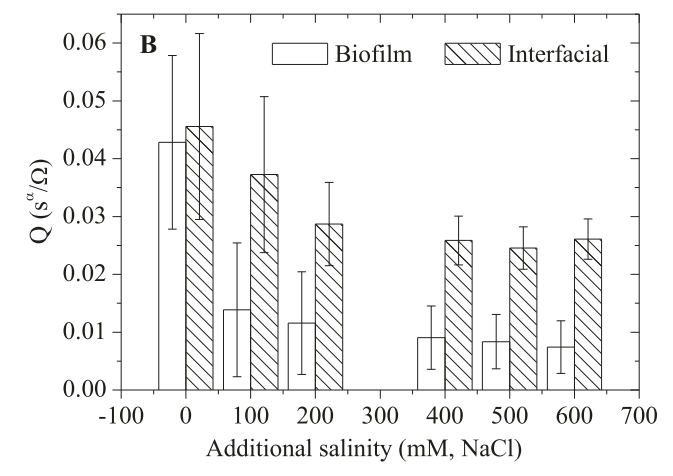


Fig. 4. Solution resistance (R1), biofilm resistance (R2) and interfacial resistance (R3) (A), and CPE coefficients (Q) (B) in PBS-buffered BES at different additional salinity, calculated from the fitting of EIS.

NaCl addition.

Biofilm resistance (R2) is the charge transfer resistance inside the EAB, which first decreases from 4.16 \pm 0.75 Ω (0 mM) to 0.94 \pm 0.21 Ω (200 mM), and then arrives at stable levels (\sim 0.5 Ω) under the last three conditions (Fig. 4A). However, current production kept decreasing even though both R1 and R2 decreased. There was 50 mM PBS in medium for all experiments, which would lead to sufficient ionic strength and accordingly favorably decrease solution resistance. So, further increased ionic strength resulting from additional salinity would not improve current production. It was reported that maximum power density slightly increased from 483 mW/m² (50 mM PBS) to 528 mW/m² (200 mM PBS) when solution conductivity increased from 7.65 mS/cm (50 mM PBS) to 14.6 mS/cm (200 mM PBS) (Feng et al., 2008). On the other hand, it has been suggested that biofilm conductivity is high enough (0.5 mS/cm) and would not limit current production (Schrott et al., 2011). More recently, a higher biofilm conductivity of 2.44 \pm 0.42 mS/ cm was observed which caused negligible maximum energy loss for ohmic-conduction extracellular electron transfer (Lee et al., 2016). Overall, high biofilm conductivity that represents the low biofilm resistance was not a decisive factor for current production in this work.

Interfacial resistance (R3) that represents the charge transfer resistance at the electrode/biofilm interface increases over the experiments, from $58.0\pm8.9\,\Omega$ (0 mM) to $82.5\pm11\,\Omega$ (600 mM) (Fig. 4A). Compared to R1 and R2, R3 was much higher, and the average contributions of R3 to the total resistance (R1 + R2 + R3) gradually increased from 85% (0 mM) to 97.8% (600 mM). It has been demonstrated that large interfacial

resistance significantly reduced power densities in MFCs (Qiao et al., 2015). Also, in a G. sulfurreducens respired BES, decreased interfacial resistance played an important role in current production enhancement (Guo et al., 2018). Increased NaCl concentrations, especially higher than 200 mM, could suppress the activities of bacteria and cytochromes as discussed above. Some cytochromes or redox mediators are essential for electron transfer from cells to the electrode, such as OmcZ in G. sulfurreducens system (Inoue et al., 2011; Richter et al., 2009), and phenazines in Pseudomonas aeruginosa respired MFC (Qiao et al., 2015). The increased interfacial resistance is due to the weakened interfacial redox reaction and poor attachment of biofilm on the electrode when the additional salt was introduced. In addition, comparable total resistances at NaCl concentrations of 0 mM (68 Ω), 100 mM (64 Ω), 200 mM (64 Ω), and 400 mM (65 Ω) were observed, indicating that the increased NaCl concentrations did not increase the total resistance, but changed the distribution of R1, R2, and R3, which influenced current production in BES. Generally, the increased interfacial resistance was the dominant reason for the gradually decreased current production.

Fig. 4B shows the changes in the CPE coefficients (Q1 and Q2), which represent the biofilm capacitance and interfacial capacitance. Both Q1 and Q2 decreased with the increase in salinity, sharing the similar changing pattern with R1 and R2. *C*-type cytochromes have been demonstrated to be responsible for the charge accumulation observed in biofilm and interfacial capacitance (Babauta and Beyenal, 2014; Schrott et al., 2011). Furthermore, previous work has shown that because of the capacitive behavior of BES, current production could be improved by intermittent polarization (Guo et al., 2018). The decreases in capacitance could be due to the inhibition of redox systems of cytochromes by the increasing NaCl concentrations, making BES less capacitive and lowered current production. In addition, Fig. 4B shows that Q2 is much higher than Q1, suggesting that charge accumulation was preferable at the biofilm/electrode interface than in the biofilm.

To sum up, decreased current production with the increase in salinity, and a negative correlation (P < 0.005) was observed. Based on CV analyses, the bacterial ability of current production of the dominant electricity-generating bacteria was not inhibited by additional salinity within 200 mM NaCl. Solution and biofilm resistances first decreased and then arrived at stable levels. Interfacial resistance gradually increased, and was suggested as the dominant reason for the decreased current production.

3.3. Acetate degradation rate and columbic efficiency

Fig. 5 shows acetate concentration in the influent and effluent, acetate removal rate, and CE at different additional salinities. Acetate concentrations in the influent slightly fluctuated from 20.9 ± 0.2 mM to 21.8 ± 0 mM. In the outlet, acetate concentrations were 5.6 ± 0.1 mM at 0 mM NaCl, experienced a slight drop to 4.8 ± 0.1 mM at 200 mM NaCl, and then gradually increased to 9.8 ± 0 mM at 600 mM NaCl. Correspondingly, acetate removal rates first increased from 1.23 ± 0.02 mol/m³/h (0 mM NaCl) to 1.38 ± 0 mol/m³/h (200 mM NaCl), then decreased to 0.98 ± 0 mol/m³/h (600 mM NaCl) (Fig. 5). In general, moderate additional salinity up to 200 mM NaCl would promote acetate removal, leading to a positive influence when BES is used for wastewater treatment. However, more than 200 mM NaCl would slow down acetate degradation, indicating a suppression of bacterial activity. Therefore, the optimal NaCl concentration for acetate removal or organic matter degradation is 200 mM ($\sim1.2\%$ NaCl, w/v) in this work.

Similar optimal salinities for COD removal were reported previously. For examples, in dual-chamber MFCs treating simulated azo dved wastewater, COD degradation efficiency first enhanced with salt content up to 1% (w/v), and a 3.3-fold decreased efficiency was observed at 2.5% salt content (Fernando et al., 2013). Adelaja et al (2015) suggested the same optimal salinity of 1% (w/v) for COD removal, which dropped rapidly with further NaCl addition. Interestingly, two pathways for organic matter degradation were proposed when chlorides were present in the substrate. One is the direct anodic oxidation (DAO) and the other is the indirect anodic oxidation (IAO) (Mohanakrishna et al., 2010). The DAO is the common degradation process for organic matter accomplished by EAB, while the IAO is by the oxidants such as chloride dioxide, hypochlorite, hydroxyl radicals and hydrogen peroxide that are bioelectrochemically generated through a similar process as happens in an electrolysis system (Israilides et al., 1997; Mohanakrishna et al., 2010). It is suggested that the IAO by the oxidants has significant influence on the organic removal efficiency (Mohanakrishna et al., 2010). So, the enhancement of acetate degradation at 200 mM NaCl probably was due to the more oxidants produced with an increased availability of chlorides. The processes and mechanisms of IAO proposed in BES are worth of further investigations.

As shown in Fig. 5, CE decreased rapidly from 17.0 \pm 0.2% (0 mM NaCl) to 9.9 \pm 0% (200 mM NaCl), and then arrived at a stable level. The

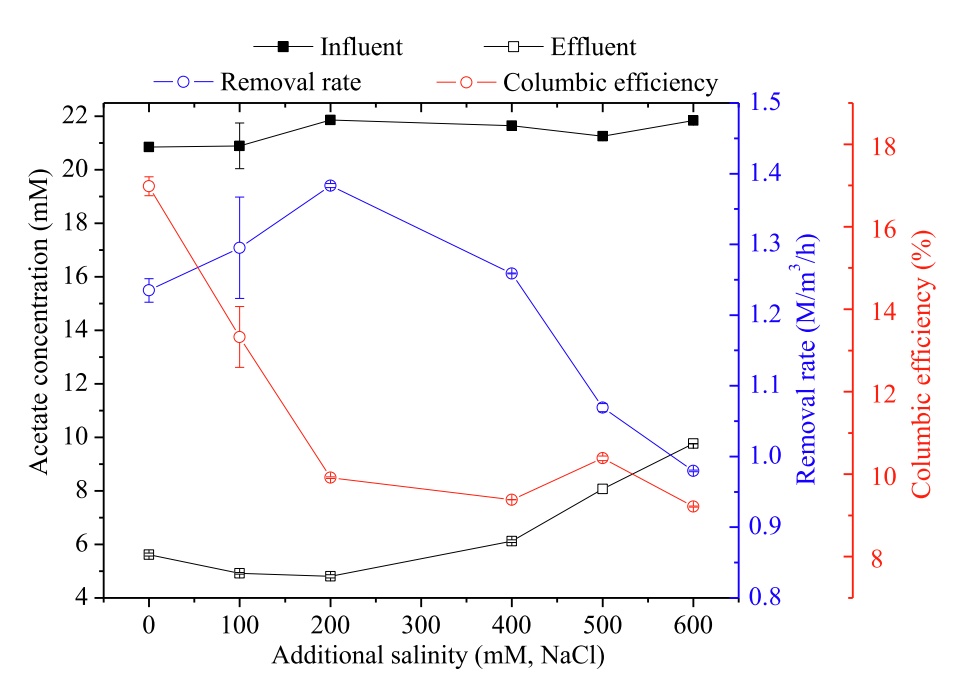


Fig. 5. Acetate concentration in the influent and effluent, acetate removal rate and columbic efficiency in PBS-buffered BES at different additional salinity.

decrease could be attributed to the lowered current production, less charge transferred and collected efficiently (Fig. 1). Furthermore, NaCl addition probably accelerate the growth of the non-electricity producing bacteria and enhance the competing metabolic processes such as fermentation (Li et al., 2013). In short, more acetate was consumed by other microorganisms than the electricity-producing bacteria, lowering the charge recovery efficiency.

4. Conclusions

In conclusion, current production decreased with increasing additional salinity from 0 to 600 mM NaCl in a PBS-buffered three-electrode BES. CV and its first derivative analyses suggested that the dominant exoelectrogens could tolerate up to 200 mM additional salinity. Increased interfacial resistance accounted for the majority of total resistance and was the controlling factor for the decreased current production. Decreases in biofilm and interfacial capacitance also contributed to the decreased current production. Optimal additional salinity for acetate degradation was 200 mM NaCl.

CRediT authorship contribution statement

Fei Guo: Funding acquisition, Conceptualization, Investigation, Writing - original draft. **Jerome T. Babauta:** Methodology, Formal analysis, Writing - review & editing. **Haluk Beyenal:** Funding acquisition, Formal analysis, Writing - review & editing.

Declaration of Competing Interest

The authors declare that they have no known competing financial interests or personal relationships that could have appeared to influence the work reported in this paper.

Acknowledgements

This research was supported by an NSF award, USA (1706889). Fei Guo acknowledges the young talents training program from Xihua University. The authors acknowledge Chloe Strupulis at the Washington State University for editing the manuscript.

References

- Adelaja, O., Keshavarz, T., Kyazze, G., 2015. The effect of salinity, redox mediators and temperature on anaerobic biodegradation of petroleum hydrocarbons in microbial fuel cells. J. Hazard. Mater. 283, 211–217.
- Babauta, J.T., Beyenal, H., 2014. Mass transfer studies of geobacter sulfurreducens biofilms on rotating disk electrodes. Biotechnol. Bioeng. 111 (2), 285–294.
- Babauta, J.T., Nguyen, H.D., Harrington, T.D., Renslow, R., Beyenal, H., 2012. pH, redox potential and local biofilm potential microenvironments within Geobacter sulfurreducens biofilms and their roles in electron transfer. Biotechnol. Bioeng. 109 (10), 2651–2662.
- Dlugolecki, P., Anet, B., Metz, S.J., Nijmeijer, K., Wessling, M., 2010a. Transport limitations in ion exchange membranes at low salt concentrations. J. Membr. Sci. 346 (1), 163–171.
- Dlugolecki, P., Ogonowski, P., Metz, S.J., Saakes, M., Nijmeijer, K., Wessling, M., 2010b. On the resistances of membrane, diffusion boundary layer and double layer in ion exchange membrane transport. J. Membr. Sci. 349 (1–2), 369–379.
- Fan, Y.Z., Sharbrough, E., Liu, H., 2008. Quantification of the internal resistance distribution of microbial fuel cells. Environ. Sci. Technol. 42 (21), 8101–8107.
- Feng, Y., Wang, X., Logan, B.E., Lee, H., 2008. Brewery wastewater treatment using aircathode microbial fuel cells. Appl. Microbiol. Biotechnol. 78 (5), 873–880.
- Fernando, E., Keshavarz, T., Kyazze, G., 2013. Simultaneous co-metabolic decolourisation of azo dye mixtures and bio-electricity generation under thermophillic (50 °C) and saline conditions by an adapted anaerobic mixed culture in microbial fuel cells. Bioresour. Technol. 127, 1–8.
- Fricke, K., Harnisch, F., Schroder, U., 2008. On the use of cyclic voltammetry for the study of anodic electron transfer in microbial fuel cells. Energy Environ. Sci. 1 (1), 144–147.
- Guo, F., Babauta, J.T., Beyenal, H., 2018. Impact of intermittent polarization on electrode-respiring Geobacter sulfurreducens biofilms. J. Power Sources 406, 96–101.

- Guo, F., Luo, H., Shi, Z., Wu, Y., Liu, H., 2020. Substrate salinity: A critical factor regulating the performance of microbial fuel cells, a review. Sci. Total Environ., 143021 https://doi.org/10.1016/j.scitotenv.2020.143021. In press.
- Harrington, T.D., Babauta, J.T., Davenport, E.K., Renslow, R.S., Beyenal, H., 2015. Excess surface area in bioelectrochemical systems causes ion transport limitations. Biotechnol. Bioeng. 112 (5), 858–866.
- Holmes, D.E., Chaudhuri, S.K., Nevin, K.P., Mehta, T., Methe, B.A., Liu, A., Ward, J.E., Woodard, T.L., Webster, J., Lovley, D.R., 2006. Microarray and genetic analysis of electron transfer to electrodes in Geobacter sulfurreducens. Environ. Microbiol. 8 (10), 1805–1815.
- Inoue, K., Leang, C., Franks, A.E., Woodard, T.L., Nevin, K.P., Lovley, D.R., 2011. Specific localization of the c-type cytochrome OmcZ at the anode surface in currentproducing biofilms of Geobacter sulfurreducens. Environ. Microbiol. Rep. 3 (2), 211–217.
- Israilides, C.J., Vlyssides, A.G., Mourafeti, V.N., Karvouni, G., 1997. Olive oil wastewater treatment with the use of an electrolysis system. Bioresour. Technol. 61 (2), 163–170
- Karthikeyan, R., Selvam, A., Cheng, K.Y., Wong, J.W.C., 2016. Influence of ionic conductivity in bioelectricity production from saline domestic sewage sludge in microbial fuel cells. Bioresour. Technol. 200, 845–852.
- Lee, H.S., Dhar, B.R., An, J., Rittmann, B.E., Ryu, H., Domingo, J.W.S., Ren, H., Chae, J., 2016. The roles of biofilm conductivity and donor substrate kinetics in a mixedculture biofilm anode. Environ. Sci. Technol. 50 (23), 12799–12807.
- Lefebvre, O., Tan, Z., Kharkwal, S., Ng, H.Y., 2012. Effect of increasing anodic NaCl concentration on microbial fuel cell performance. Bioresour. Technol. 112, 336–340.
- Li, X.M., Cheng, K.Y., Wong, J.W.C., 2013. Bioelectricity production from food waste leachate using microbial fuel cells: effect of NaCl and pH. Bioresour. Technol. 149, 452-458
- Liu, G.L., Yates, M.D., Cheng, S.A., Call, D.F., Sun, D., Logan, B.E., 2011. Examination of microbial fuel cell start-up times with domestic wastewater and additional amendments. Bioresour. Technol. 102 (15), 7301–7306.
- Liu, H., Cheng, S.A., Logan, B.E., 2005. Power generation in fed-batch microbial fuel cells as a function of ionic strength, temperature, and reactor configuration. Environ. Sci. Technol. 39 (14), 5488–5493.
- Lloyd, J.R., Leang, C., Myerson, A.L.H., Coppi, M.V., Cuifo, S., Methe, B., Sandler, S.J., Lovley, D.R., 2003. Biochemical and genetic characterization of PpcA, a periplasmic c-type cytochrome in Geobacter sulfurreducens. Biochem. J 369, 153–161.
- Logan, B.E., Rabaey, K., 2012. Conversion of wastes into bioelectricity and chemicals by using microbial electrochemical technologies. Science 337 (6095), 686–690.
- Lusk, B.G., Parameswaran, P., Popat, S.C., Rittmann, B.E., Torres, C.I., 2016. The effect of pH and buffer concentration on anode biofilms of Thermincola ferriacetica. Bioelectrochemistry 112, 47–52.
- Magnuson, T.S., Isoyama, N., Hodges-Myerson, A.L., Davidson, G., Maroney, M.J., Geesey, G.G., Lovley, D.R., 2001. Isolation, characterization and gene sequence analysis of a membrane-associated 89 kDa Fe(III) reducing cytochrome c from Geobacter sulfurreducens. Biochem. J 359, 147–152.
- Marsili, E., Rollefson, J.B., Baron, D.B., Hozalski, R.M., Bond, D.R., 2008. Microbial biofilm voltammetry: direct electrochemical characterization of catalytic electrodeattached biofilms. Appl. Environ. Microbiol. 74 (23), 7329–7337.
- Miyahara, M., Kouzuma, A., Watanabe, K., 2015. Effects of NaCl concentration on anode microbes in microbial fuel cells. Amb. Express 5, 34.
- Miyahara, M., Kouzuma, A., Watanabe, K., 2016. Sodium chloride concentration determines exoelectrogens in anode biofilms occurring from mangrove-grown brackish sediment. Bioresour. Technol. 218, 674–679.
- Mohanakrishna, G., Mohan, S.V., Sarma, P.N., 2010. Bio-electrochemical treatment of distillery wastewater in microbial fuel cell facilitating decolorization and desalination along with power generation. J. Hazard. Mater. 177 (1–3), 487–494.
- Nam, J.Y., Kim, H.W., Lim, K.H., Shin, H.S., Logan, B.E., 2010. Variation of power generation at different buffer types and conductivities in single chamber microbial fuel cells. Biosens. Bioelectron. 25 (5), 1155–1159.
- Nevin, K.P., Kim, B.C., Glaven, R.H., Johnson, J.P., Woodard, T.L., Methe, B.A., DiDonato, R.J., Covalla, S.F., Franks, A.E., Liu, A., Lovley, D.R., 2009. Anode biofilm transcriptomics reveals outer surface components essential for high density current production in Geobacter sulfurreducens fuel cells. PLoS One 4 (5), e5628.
- Oliot, M., Galier, S., de Balmann, H.R., Bergel, A., 2016. Ion transport in microbial fuel cells: key roles, theory and critical review. Appl. Energy 183, 1682–1704.
- Patil, S.A., Harnisch, F., Kapadnis, B., Schroder, U., 2010. Electroactive mixed culture biofilms in microbial bioelectrochemical systems: the role of temperature for biofilm formation and performance. Biosens. Bioelectron. 26 (2), 803–808.
- Pessanha, M., Morgado, L., Louro, R.O., Londer, Y.Y., Pokkuluri, P.R., Schiffer, M., Salgueiro, C.A., 2006. Thermodynamic characterization of triheme cytochrome PpcA from Geobacter sulfurreducens: evidence for a role played in e(-)/H+ energy transduction. Biochemistry 45 (46), 13910–13917.
- Pierra, M., Carmona-Martinez, A.A., Trably, E., Godon, J.J., Bernet, N., 2015. Specific and efficient electrochemical selection of Geoalkalibacter subterraneus and Desulfuromonas acetoxidans in high current-producing biofilms. Bioelectrochemistry 106, 221–225.
- Qiao, Y., Qiao, Y.J., Zou, L., Ma, C.X., Liu, J.H., 2015. Real-time monitoring of phenazines excretion in Pseudomonas aeruginosa microbial fuel cell anode using cavity microelectrodes. Bioresour. Technol. 198, 1–6.
- Richter, H., Nevin, K.P., Jia, H.F., Lowy, D.A., Lovley, D.R., Tender, L.M., 2009. Cyclic voltammetry of biofilms of wild type and mutant Geobacter sulfurreducens on fuel cell anodes indicates possible roles of OmcB, OmcZ, type IV pili, and protons in extracellular electron transfer. Energy Environ. Sci. 2 (5), 506–516.

- Rousseau, R., Dominguez-Benetton, X., Delia, M.L., Bergel, A., 2013. Microbial bioanodes with high salinity tolerance for microbial fuel cells and microbial electrolysis cells. Electrochem. Commun. 33, 1–4.
- Rousseau, R., Santaella, C., Achouak, W., Godon, J.J., Bonnafous, A., Bergel, A., Delia, M. L., 2014. Correlation of the electrochemical kinetics of high-salinity-tolerant bioanodes with the structure and microbial composition of the biofilm. Chemelectrochem 1 (11), 1966–1975.
- Schrott, G.D., Bonanni, P.S., Robuschi, L., Esteve-Nunez, A., Busalmen, J.P., 2011. Electrochemical insight into the mechanism of electron transport in biofilms of Geobacter sulfurreducens. Electrochim. Acta 56 (28), 10791–10795.
- Seeliger, S., Cord-Ruwisch, R., Schink, B., 1998. A periplasmic and extracellular c-type cytochrome of Geobacter sulfurreducens acts as a ferric iron reductase and as an electron carrier to other acceptors or to partner bacteria. J. Bacteriol. 180 (14), 3686–3691.
- Srikanth, S., Marsili, E., Flickinger, M.C., Bond, D.R., 2008. Electrochemical characterization of Geobacter sulfurreducens cells immobilized on graphite paper electrodes. Biotechnol. Bioeng. 99 (5), 1065–1073.

- Tan, F.X., Zhang, L.H., Liu, W.F., Zhu, Y.M., 2019. Osmotic pressure compensated solute ectoine improves salt tolerance of microbial cells in microbial fuel cells. Fuel Cells 19 (5), 616–622.
- Torres, C.I., Marcus, A.K., Rittmann, B.E., 2008. Proton transport inside the biofilm limits electrical current generation by anode-respiring bacteria. Biotechnol. Bioeng. 100 (5), 872–881.
- Vijay, A., Arora, S., Gupta, S., Chhabra, M., 2018. Halophilic starch degrading bacteria isolated from Sambhar Lake, India, as potential anode catalyst in microbial fuel cell: a promising process for saline water treatment. Bioresour. Technol. 256, 391–398.
- Wang, X., Cheng, S.A., Zhang, X.Y., Li, X.Y., Logan, B.E., 2011. Impact of salinity on cathode catalyst performance in microbial fuel cells (MFCs). Int. J. Hydrogen Energy 36 (21), 13900–13906.
- Zeng, F.J., Wu, Y.T., Bo, L., Zhang, L.H., Liu, W.F., Zhu, Y.M., 2020. Coupling of electricity generation and denitrification in three-phase single-chamber MFCs in high-salt conditions. Bioelectrochemistry 133, 107481.
- Zuo, Y., Maness, P.C., Logan, B.E., 2006. Electricity production from steam-exploded corn stover biomass. Energy Fuels 20 (4), 1716–1721.